Hindawi
International Journal of Chemical Engineering
Volume 2021, Article ID 5520448, 9 pages
https://doi.org/10.1155/2021/5520448

Research Article

The Effect of Ultraviolet Wavelength on Corrosion Behavior of 7075 Aluminum Alloy in the Marine Atmospheric Environment

Yanyu Cui, Yuning Gao, Yongxiang Qin, and Xiaoyu Shi

College of Airport, Civil Aviation University of China, Tianjin, China

Correspondence should be addressed to Yuning Gao; 1365331633@qq.com

Received 27 January 2021; Revised 27 March 2021; Accepted 22 April 2021; Published 29 April 2021

Academic Editor: Chuanxi Yang

The influence of ultraviolet rays on the corrosion behavior of 7075 aluminum alloy in the marine atmosphere was studied by salt spray corrosion test. Electrochemical methods and surface analysis techniques were used to analyze and compare the corrosion laws of 7075 aluminum alloy in the marine atmosphere under ultraviolet radiation with wavelengths of 0 nm, 185 nm, 254 nm, and 365 nm. The results showed that ultraviolet light irradiation could promote the corrosion of 7075 aluminum alloy. Oxygen was prone to chemical reactions to form oxygen atoms after being irradiated by ultraviolet rays, and oxygen atoms recombined with oxygen to form ozone in the marine atmosphere. The 7075 aluminum alloy in the marine atmosphere accelerated corrosion due to the increasing ozone content. Although there were passivation films with different degrees of protection on the surface of aluminum alloy under ultraviolet irradiation, the surface of 7075 aluminum alloy in the marine atmosphere failed to form a stable passivation film after pitting, and the corrosion rate was the fastest when the ultraviolet wavelength was 185 nm.

1. Introduction

7075 aluminum alloy is an ultrahigh-strength deformed aluminum alloy. Because of its good mechanical properties, it is often used as a material for high-strength accessories. In the late 1940s, the 7000-series aluminum alloy was used in the aircraft manufacturing industry, and it is still widely used in the aviation industry until now. 7075 aluminum alloy is used as an aircraft frame material due to its good corrosion resistance [1]. However, 7075 aluminum alloy materials also underwent severe corrosion in specific environments such as high salt and high humidity. The International Air Transport Association clearly pointed out that the corrosion was one of the main factors of aircraft failures.

In the marine atmosphere, harsh high-temperature environment, and high humidity, ultraviolet rays could cause pitting corrosion, intergranular corrosion, and exfoliation corrosion on the aluminum alloy surface in turn [2]. Some scholars used SEM, XRD, electrochemical testing techniques, Fourier-transform infrared spectroscopy (FTIR), and X-ray diffraction to investigate the corrosion behavior of aluminum alloys [3–5]. The main experimental methods included atmospheric exposure experiments, laboratory tests, and software simulations. The corrosion behavior of aluminum alloy in the coastal environment, high-temperature and high-humidity environment, and strong sunlight environment was studied. The researchers pointed out that the factors affecting the corrosion of aluminum alloys include the time of corrosion, atmospheric temperature, relative humidity, salt content, alternating dry and wet environments, air pollution, and light intensity [6–11]. Atmospheric corrosion of metallic aluminum under natural conditions was caused by the combination of pollutants such as H_2S, Cl^-, SO_2, SO_3, NO_x, CO_2, and O_3 and meteorological conditions [12, 13]. The process was more complicated.

When flying over the ocean, the aircraft will suffer from atmospheric corrosion and seawater erosion. The surface of the aircraft flying at high altitudes will also be exposed to strong ultraviolet radiation. In this paper, 7075 aluminum alloy aircraft skin was used as an experimental sample to study the metal corrosion phenomenon of the aircraft surface caused by the marine atmosphere. Electrochemical methods and surface analysis techniques were used to compare the corrosion behavior of 7075 aluminum alloys

irradiated by ultraviolet rays with wavelengths of 0 nm, 185 nm, 254 nm, and 365 nm. The research results would provide a theoretical basis for the corrosion protection of the aluminum alloy of the aircraft fuselage flying at high altitudes over the ocean.

2. Materials and Methods

2.1. Experimental Sample. We used 7075 aluminum alloy as the working electrode in the experiment. The materials used in the experiment were provided by Mingtai Aluminum Industry. The chemical composition (mass fraction) of the 7075 aluminum alloy is shown in Table 1. The size of the samples was 20 mm × 20 mm × 3 mm. The back of the samples was welded with a copper wire, and the other side was used as the experimental working surface. The non-working surface of the sample was sealed with epoxy resin. The working surface area was 400 mm^2, as shown in Figure 1.

We polished the sample surface with a series of sandpaper up to 2000# until there was no obvious scratch on the sample surface. The working face was rinsed successively with acetone, absolute alcohol, and distilled water. And then, we dried and weighed the samples (digital balance has an accuracy of 0.1 mg) before using.

2.2. Experimental Device. The experimental device used in this experiment is shown in Figure 2 [14]. A mass flow controller was installed at the entrance to adjust the air flow rate so that the air flow maintained a constant flow rate and entered the experimental device. The air flowed in through the air pump device, and the air flowing out of the flow controller flowed through the saturated solution and two drying tanks in sequence to undergo deacidification and dry treatments, respectively. The deacidified and dried air entered the sealed box. Inside the sealed box, there was a partition with a small hole to place the sample, and the top was equipped with a UV lamp with adjustable wavelength, which could be irradiated vertically from the sample. The bottom of the sealed box was a simulated seawater solution. Seawater used in the experiment was configured according to ASTM D1141-1998(2013), and the chemical composition is listed in Table 2.

2.3. Experimental Method

2.3.1. Weightlessness Method. After the salt spray test for 28 days, the samples were taken out and rinsed with running water. The rust-removing solution was used to remove the corrosion products on the surface of the samples. The samples were fully dried until the differences between the two measurements were within 0.0002 g, and then they were weighed again with an electronic balance. The corrosion rate was calculated by the mass loss of the samples before and after corrosion.

2.3.2. Electrochemical Test. The CHI660D electrochemical workstation was used to measure the electrochemical parameters of the samples. The three-electrode test system was used in the measurement process. The saturated calomel electrode was used as the reference electrode, the 7075 aluminum alloy sample was the working electrode, and the Pt electrode was the auxiliary electrode. Electrochemical test mainly included open-circuit potential (OCP), potential polarization curve (Tafel), and alternating current impedance (EIS) test. The specific operation was as follows: first, we performed an open-circuit potential test on the working electrode and performed the potential dynamic polarization curve test after the open-circuit potential value was stable. The scan rate was 0.1 mV/s, and the scan range was Eocp ± 250 mV. During the AC impedance (EIS) test, the sweep rate was adjusted to 0.5 mV/s, the test frequency range was 10^{-2}~10^{6} Hz, and the AC excitation signal was a sine wave of 10 mV.

Table 1: Chemical composition of 7075 aluminum alloy (%).

Si	Fe	Cu	Mn	Mg	Cr	Zn	Ti	Al
0.40	0.50	1.2–2.0	0.30	2.1–2.9	0.18–0.28	4.49	0.20	Balance

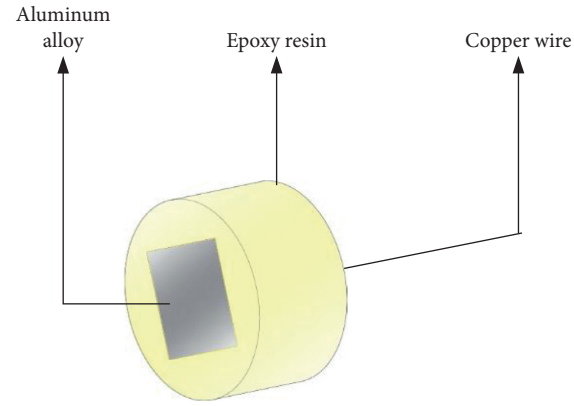

Figure 1: 7075 aluminum alloy electrode sample.

2.3.3. Surface Morphology. We analyzed the surface of the samples after corrosion. ZEISS (EVO MA15) scanning electron microscope was used to analyze the microscopic morphology (SEM) of the sample surface, and the scanning voltage was 20 kV.

3. Results and Discussion

3.1. Surface Corrosion Morphology. Figure 3 shows the morphology of the 7075 aluminum alloy sample before corrosion.

It can be seen from Figure 3 that the surface of the sample that has not been corroded was relatively flat.

Figure 4 shows the surface corrosion morphology of 7075 aluminum alloy samples after being irradiated by different wavelengths of ultraviolet rays in the simulated ocean atmosphere. Figures 4(a)–4(d) correspond to the corrosion morphology of the 7075 aluminum alloy irradiated by ultraviolet rays with wavelengths of 0 nm (dark environment, recorded as 0 nm), 185 nm, 254 nm, and 365 nm for 28 days, respectively.

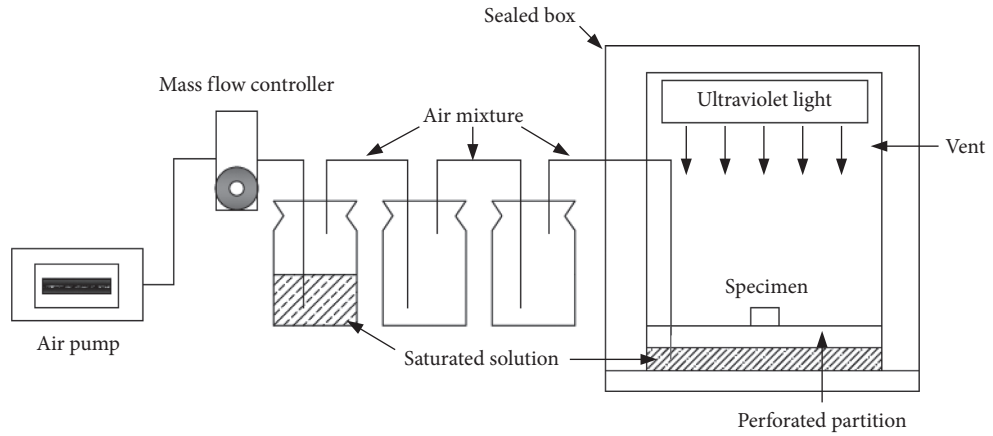

Figure 2: Sketch of the experimental device model.

Table 2: Simulation of the specific composition of seawater solution (%).

NaCl	$MgCl_2$	Na_2SO_4	$CaCl_2$	KCl	$NaHCO_3$	KBr	H_3BO_3	$SrCl_2$	NaF
24.530 g/L	5.200 g/L	4.090 g/L	1.160 g/L	0.695 g/L	0.201 g/L	0.101 g/L	0.027 g/L	0.025 g/L	0.003 g/L

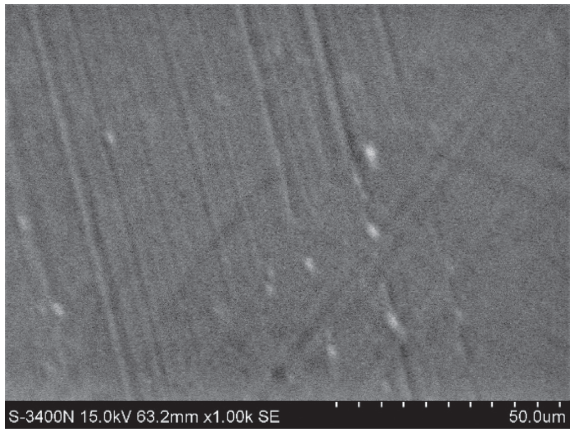

Figure 3: The morphology of the 7075 aluminum alloy sample before corrosion.

It can be seen from Figure 4(a) that when the ultraviolet wavelength was 0 nm, the corrosion product layer on the surface of 7075 aluminum alloy was thinner, the overall corrosion product was relatively small, and the corrosion degree of the sample surface was lighter. It can be seen from Figure 4(b) that there were dense corrosion pits on the surface of the sample irradiated by ultraviolet light with a wavelength of 185 nm, and the surface of the sample was severely corroded. On the one hand, because the corrosion products formed on the surface of 7075 aluminum alloy fell off under the condition of 185 nm ultraviolet radiation, the surface of the substrate was further in contact with the ocean atmosphere, which promotes the corrosion of 7075 aluminum alloy. On the other hand, in a high-salt and high-humidity environment, the corrosion pits formed on the surface of 7075 aluminum alloy form crevice corrosion, which further accelerated the corrosion of the metal matrix. It can be seen from Figure 4(c) that when the ultraviolet wavelength was 254 nm, a large number of corrosion products appeared on the surface of 7075 aluminum alloy, and a dense layer of corrosion products was formed. Therefore, compared with the 185 nm ultraviolet radiation environment, under the action of the corrosion product film, the corrosion rate of 7075 aluminum alloy after being irradiated by ultraviolet rays with wavelengths of 254 nm and 365 nm would be reduced. It can be seen from Figure 4(d) that when the ultraviolet wavelength was 365 nm, a corrosion product film was also formed on the surface of 7075 aluminum alloy, but compared with the 254 nm ultraviolet environment, the corrosion products were relatively less, indicating that the corrosion degree of 7075 aluminum alloy was further slowed down.

Therefore, ultraviolet rays with a wavelength of 185 nm would cause corrosion products on the surface of 7075 aluminum alloy to fall off, and the corrosion product layer covered on the surface presents a porous structure. This

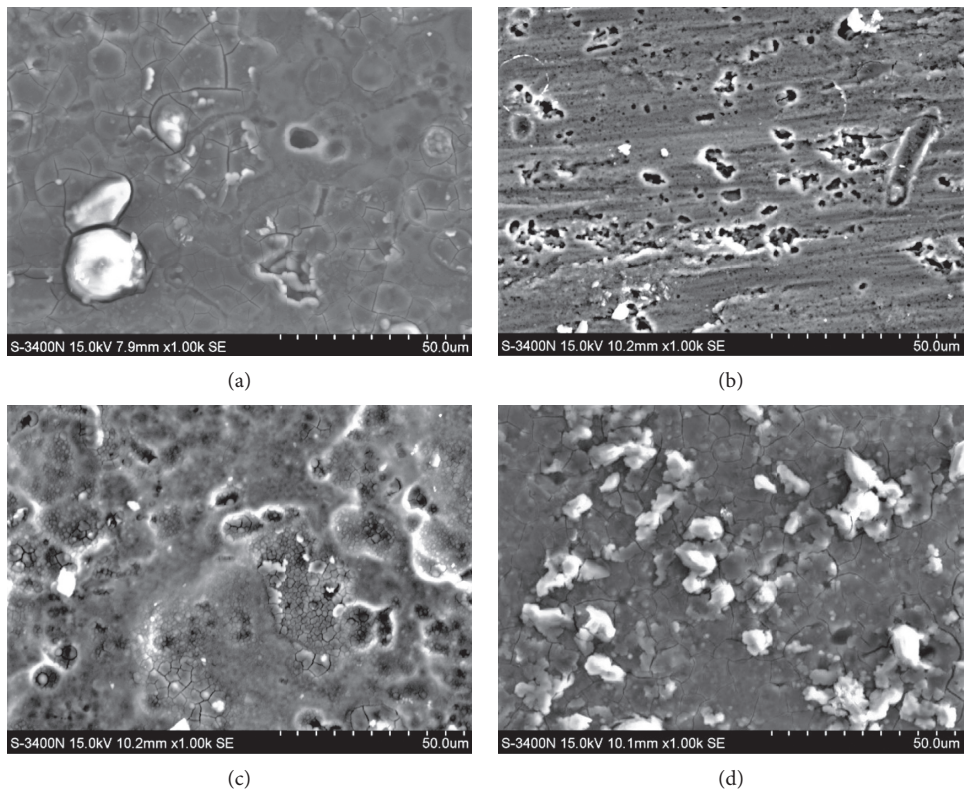

Figure 4: Corrosion morphology of 7075 aluminum alloy irradiated by different wavelengths of ultraviolet rays. (a) 0 nm. (b) 185 nm. (c) 254 nm. (d) 365 nm.

phenomenon might cause the specimens irradiated with ultraviolet rays with a wavelength of 185 nm to be more prone to corrosion than specimens irradiated with ultraviolet rays with a wavelength of 254 nm and 365 nm.

3.2. Weightlessness Experiment Analysis. The corrosion rate of 7075 aluminum alloy samples exposed to different wavelengths of ultraviolet rays in the marine atmosphere was measured and calculated by the weightlessness experiment method. The corrosion rate was expressed by mass change, and the relationship curve between the corrosion rate of the sample and the ultraviolet wavelength was obtained. In order to reduce the error, the mass change values of three samples were measured under corresponding conditions. The result is shown in Figure 5.

It can be seen from Figure 5 that the corrosion rate of the samples irradiated by ultraviolet rays was obviously greater than that of the samples with no ultraviolet rays. And due to different wavelengths of ultraviolet radiation, the corrosion rate of 7075 aluminum alloy was also different. Ultraviolet rays with a wavelength of 185 nm had the greatest impact on the corrosion of the sample surface, and they led to accelerated corrosion. The corrosion rate of 7075 aluminum alloy irradiated by ultraviolet rays with a wavelength of 365 nm was lower than that of 185 nm and 254 nm. It can be seen from the corrosion rate data in Figure 5 that, in the same corrosion environment, the corrosion rate of the samples was increased by 2 to 3 times due to ultraviolet radiation, but for the samples irradiated with different

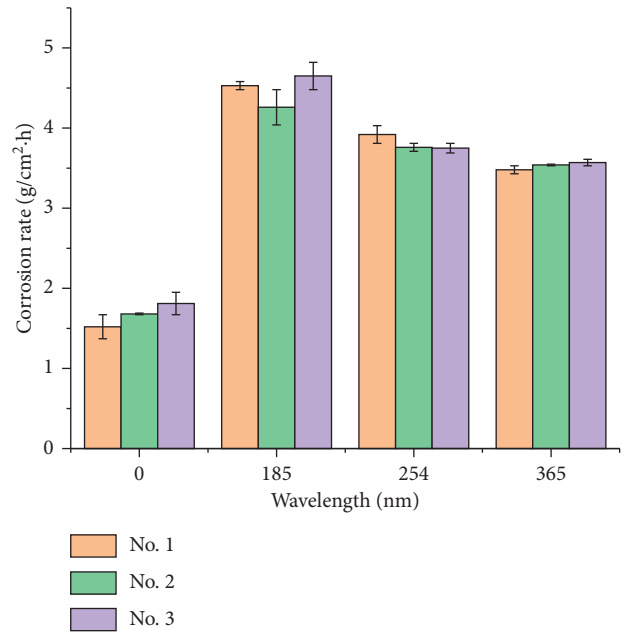

Figure 5: The relationship between the corrosion rate of the 28 d sample and the ultraviolet wavelength.

wavelengths of ultraviolet light, the corrosion rate did not increase with the increase of ultraviolet wavelength. The mass loss of samples irradiated by ultraviolet light with a wavelength of 185 nm was greater than that of samples with wavelengths of 254 nm and 365 nm.

3.3. Electrochemical Behavior

3.3.1. Analysis of Polarization Curves. The 7075 aluminum alloy samples were placed in the experimental device to simulate the corrosion accompanied by ultraviolet radiation in the marine atmosphere. Figures 6(a)–6(d), respectively, correspond to the polarization curves of 7075 aluminum alloy irradiated by ultraviolet rays with wavelengths of 0 nm, 185 nm, 254 nm, and 365 nm in different periods.

It can be found from the polarization curves in Figure 6 that the self-corrosion potential of the metal sample surface was affected by the corrosion time. As the corrosion time increased, the self-corrosion potential of the sample increased. The experimental results showed that the self-corrosion potential of the sample surface was highest on the 28th day. As shown in Figure 6, there were three curves (the curve of the sample at the 1st day with no ultraviolet radiation (a), the curve at the 28th day with 254 nm ultraviolet wavelength (c), and the curve at the 1st day with 365 nm ultraviolet wavelength (d)) which showed that the current density in the anode area increased sharply and finally stabilized, which was the characteristic of steady-state pitting and passivation. When the ultraviolet wavelength was 185 nm, the polarization curves of 1 d, 21 d, and 28 d only showed a sudden increase in current density without obvious passivation platform. It showed that 7075 aluminum alloy underwent obvious pitting corrosion in the marine atmosphere and produced a passivation film that could inhibit the continued development of metal corrosion. However, when 7075 aluminum alloy samples were irradiated by ultraviolet rays with a wavelength of 185 nm, the surface failed to form a stable passivation film after pitting.

Figure 7 shows the polarization curves of the samples after 28 days of irradiation with ultraviolet rays of different wavelengths. The surface current density and potential curves of the sample in Figure 7 were fitted and processed to obtain the relevant electrochemical parameter values, as shown in Table 3. The parameters in Table 3 were used to analyze and compare the corrosion behavior of 7075 aluminum alloy in the marine atmosphere under different wavelengths of ultraviolet radiation.

It can be seen from Figure 7 that the surface self-corrosion potential of the 7075 aluminum alloy sample was different due to the change of ultraviolet wavelength after 28 days of corrosion. When the ultraviolet wavelength was 185 nm, the current density on the metal surface was the highest. As shown in Table 3, it can be found that when the ultraviolet wavelength was 185 nm, the surface current density i_{corr} of the sample was the largest. The conclusion was consistent with the results obtained by the weightlessness method. Therefore, ultraviolet rays with a wavelength of 185 nm had the greatest impact on the corrosion behavior of 7075 aluminum alloy in the marine atmosphere, and the corrosion rate was the largest.

3.3.2. Analysis of EIS. The AC impedance diagrams were used to analyze the corrosion resistance of the materials. The impedance of the materials was analyzed by comparing the shapes of the capacitive reactance arc in the impedance spectrum. The larger the arc, the greater the impedance and the better the corrosion resistance of the material [15, 16]. Figure 8 shows the electrochemical impedance spectra of samples irradiated by ultraviolet rays of different wavelengths in the ocean atmosphere for 28 days.

It can be seen from Figure 8 that, after 28 days of ultraviolet radiation irradiated in the marine atmosphere, the curve shapes of the samples in the electrochemical impedance spectrum were a single capacitive reactance arc. The capacitance arc of the specimens irradiated by different wavelengths of ultraviolet rays was different. The diameter of the capacitive reactance arc in electrochemical impedance spectroscopy represented the resistance during charge transfer, so the size of the capacitive reactance arc had an inverse relationship with the corrosion rate. Figure 8 shows that the electrochemical impedance spectroscopy capacitance arc of the sample was the smallest when the ultraviolet wavelength was 185 nm, and the metal had poor corrosion resistance at this time.

According to the corrosion process of the sample and its surface corrosion morphology, we combined with the basic principles of aluminum alloy corrosion, and the equivalent circuit model finally selected in this experiment is shown in Figure 9. C_1 represents the capacitance of the corrosion product film on the sample surface. C_2 represents the capacitance of the chemical reaction double layer between the sample and the reaction medium. R_r represents the resistance of the reaction medium, R_t the resistance of the oxide film and corrosion products on the surface of the metal sample, and R_s represents the resistance experienced during the charge transfer process when the electrochemical reaction occurred.

ZSimpwin software was used to fit the parameters in the equivalent circuit diagram of 7075 aluminum alloy corrosion in the marine atmosphere. Figure 10 shows the data of each component in the equivalent circuit diagram.

As shown in Figure 10, it can be concluded that when there was no ultraviolet radiation, the resistance during the charge transfer during the reaction was 558.8 $\Omega \cdot cm^2$, and the charge transfer resistance was 73.08 $\Omega \cdot cm^2$ under ultraviolet rays with a wavelength of 185 nm for the test. The corrosion rate of the sample without the irradiation of ultraviolet light was the smallest. When the ultraviolet wavelength was 185 nm, the resistance of the electrochemical reaction electron migration was the smallest, and the corrosion rate of the sample was the largest. The ultraviolet radiation could reduce the surface charge transfer resistance of the sample, and the corrosion rate would increase accordingly, consistent with the results measured by the weightlessness method.

It can be seen from Figure 10 that the resistance of the reaction medium was the smallest in an environment without ultraviolet radiation. The resistance of the reaction medium increased significantly under ultraviolet light with wavelengths of 185 nm, 254 nm, and 365 nm. Therefore, ultraviolet radiation could increase the resistance of the medium in the marine atmosphere, and the resistance of the reaction medium was the largest in the test environment where the ultraviolet wavelength was 365 nm.

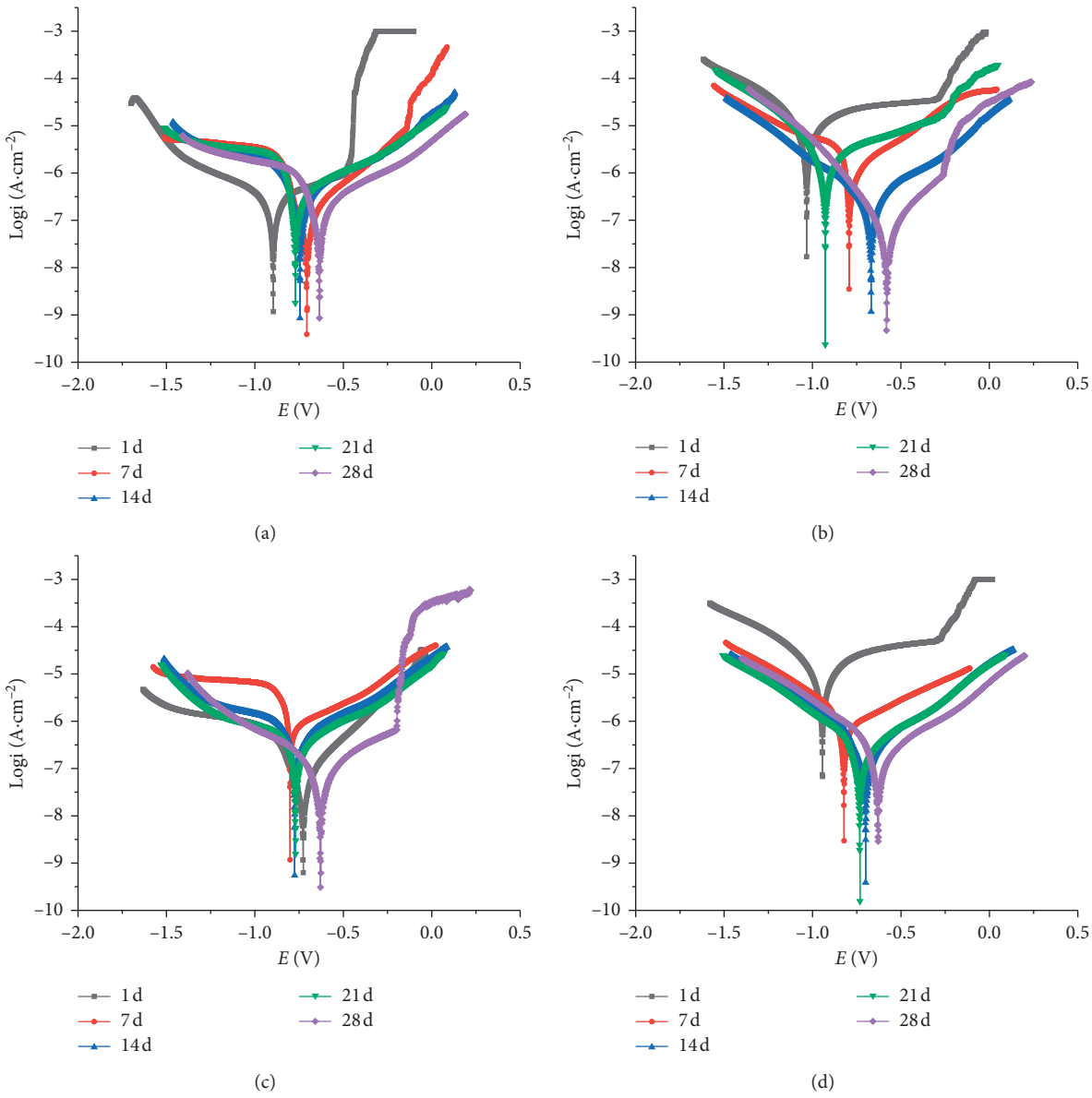

FIGURE 6: The polarization curves of the sample for different days after the corresponding wavelength UV irradiation. (a) 0 nm. (b) 185 nm. (c) 254 nm. (d) 365 nm.

3.4. Corrosion Mechanism Research. Many scholars believed that the most important factor affecting corrosion in the marine atmosphere was Cl^- in seawater and the atmosphere. A large number of experimental data proved that Cl^- had a promoting effect on metal corrosion [17–20]. Regarding the main chemical reactions of metallic aluminum in the ocean atmosphere, scholars have reached the same conclusion [5, 21, 22]. The corrosion of metallic aluminum in the atmosphere was considered to be electrochemical corrosion. This chemical reaction directly promoted the thinning of the oxide film or the fracture of the metal, and even the aluminum alloy matrix was dissolved [20].

$$\begin{aligned} &\text{Anode reaction}: Al - 3e \longrightarrow Al^{3+} \\ &\text{Cathodic reaction}: O_2 + 2H_2O + 4e \longrightarrow 4OH^- \end{aligned} \quad (1)$$

A large amount of Cl^- in the ocean atmosphere participated in the reaction. Cl^- would be adsorbed on the surface of aluminum alloy and chemically reacted with the oxide film on the metal surface. After a series of reactions, the final $AlCl_3$ product soluble in water was obtained. The specific reaction steps are as follows:

$$\begin{aligned} Al(OH)3 + Cl^- &\longrightarrow Al(OH)_2Cl + OH^- \\ Al(OH)_2Cl + Cl^- &\longrightarrow Al(OH)Cl_2 + OH^- \\ Al(OH)Cl_2 + Cl^- &\longrightarrow AlCl_3 + OH^- \end{aligned} \quad (2)$$

For metals irradiated by ultraviolet rays, the corrosion might also be affected by other factors. For example, oxygen underwent a corresponding chemical reaction under the irradiation of a certain wavelength of ultraviolet light to

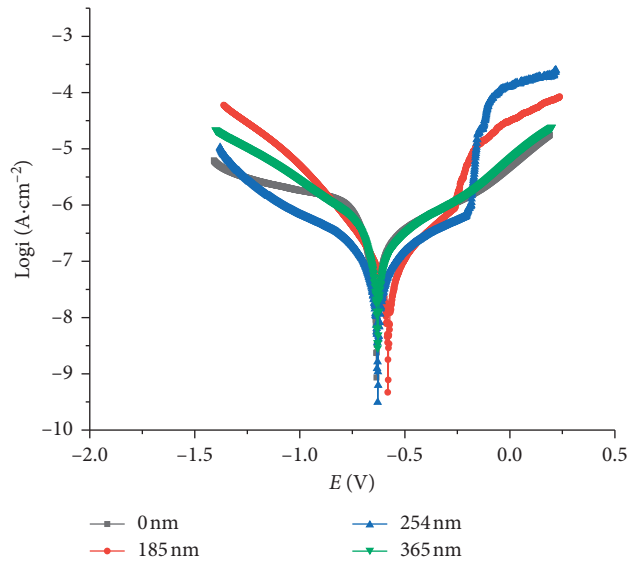

Figure 7: Polarization curves of samples after 28 days of ultraviolet irradiation with different wavelengths.

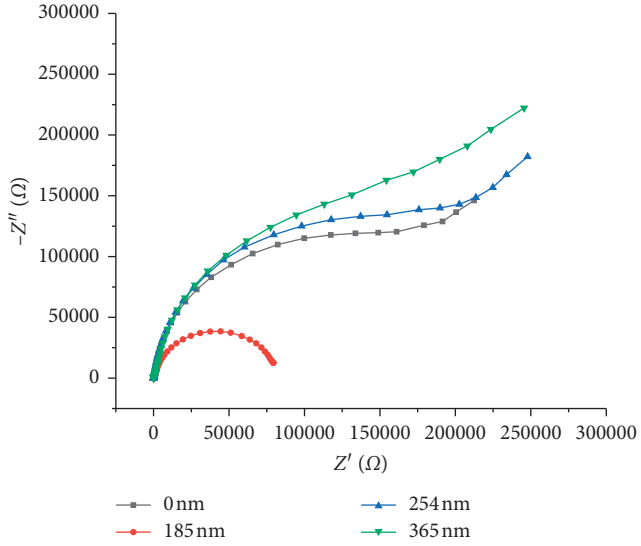

Figure 8: Electrochemical impedance spectroscopy of aluminum alloy samples under different wavelengths of ultraviolet for 28 days.

Table 3: The fitting results of the kinetic parameters of the polarization curve of the sample after 28 days of ultraviolet irradiation with different wavelengths.

Wavelength (nm)	E_{corr} (V)	i_{corr} (μA/cm^2)	β_a (mV·dec^{-1})	β_c (mV·dec^{-1})
0	−0.635	251.75	887.30	648.95
185	−0.651	482.0	767.89	658.77
254	−0.629	152.9	715.50	701.39

generate oxygen atoms [23]; the recombination of oxygen atoms and oxygen molecules generated ozone.

The conversion process of oxygen and ozone under ultraviolet radiation is as follows:

$$\begin{aligned} O_2 + h\nu &\longrightarrow O + O \\ O_2 + O &\longrightarrow O_3 \end{aligned} \quad (3)$$

h is Planck's constant, a physical constant that described the size of a quantum; ν is the frequency of ultraviolet light.

O_3 usually had a catalytic acceleration effect on metal corrosion. O_3 would react with H^+ and Cl^- on the metal surface. On the contrary, the interaction of oxygen atoms with water molecules in the air generated OH radicals to increase the corrosiveness of the atmosphere [24], thereby significantly increasing the corrosion rate of metals. This also

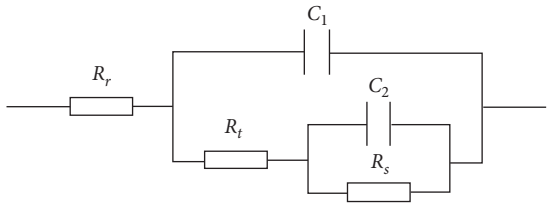

Figure 9: Equivalent circuit.

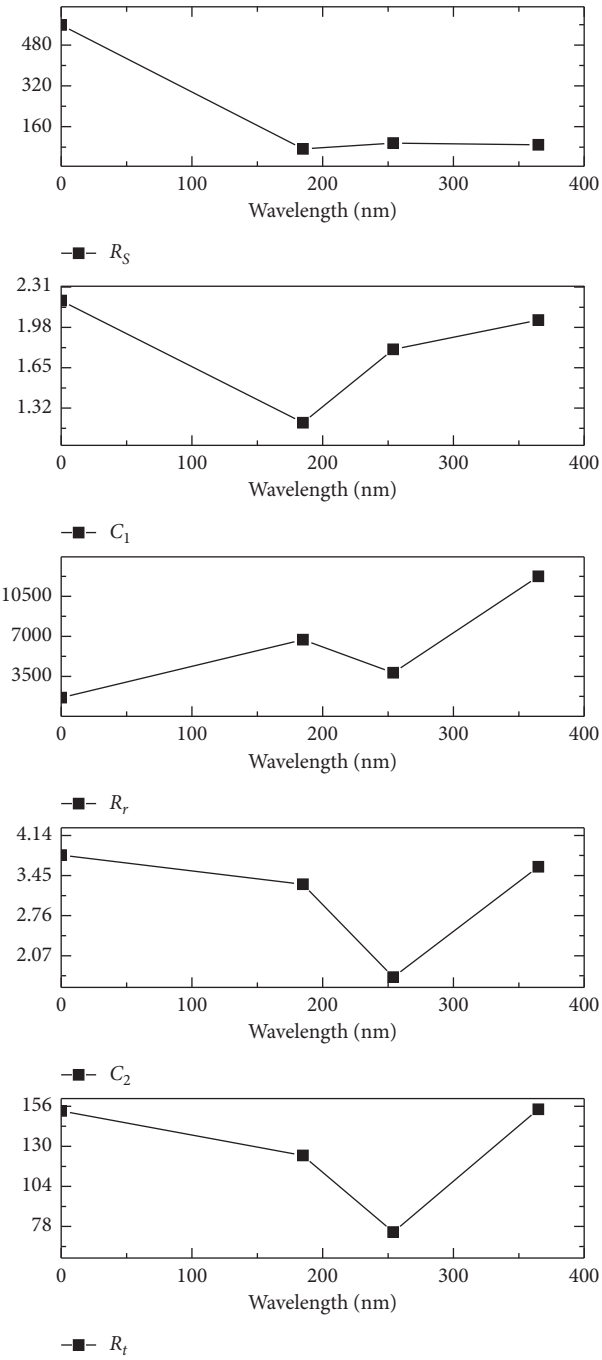

Figure 10: Component parameters in the equivalent circuit diagram.

explained why the corrosion rate of 7075 aluminum alloy specimens under ultraviolet light irradiation was faster than that of specimens without ultraviolet light irradiation.

4. Conclusions

(1) The corrosion rate of 7075 aluminum alloy in the marine atmosphere could increase significantly due to ultraviolet radiation. The corrosion rate of the specimen irradiated by ultraviolet light is 2 to 3 times greater than that of the specimen without ultraviolet light.

(2) For the 7075 aluminum alloy sample in the marine atmosphere, the surface corrosion could increase when exposed to ultraviolet rays. When the ultraviolet wavelength is 185 nm, the corrosion products on the sample surface are arranged loosely and have more pores. When the wavelength is 254 nm and 365 nm, the corrosion products on the sample surface are distributed more uniformly and have fewer pores.

(3) For different wavelengths of ultraviolet radiation, the corrosion rate of 7075 aluminum alloy in the marine atmosphere is different. The 7075 aluminum alloy in the marine atmosphere failed to form a stable passivation film after being pitted under the ultraviolet wavelength of 185 nm, and the corrosion rate is the fastest.

Data Availability

The research data used to support the findings of this study are included within the article.

Conflicts of Interest

The authors declare that there are no conflicts of interest regarding the publication of this article.

Acknowledgments

This research work was supported by Civil Aviation Safety Capacity Building Fund (Construction of safety evaluation system for multibranch complex annular apron pipe network).

References

[1] H. Ji, "Development and application of 7000 high strength aluminum alloys on airplane," *Aeronautical Science & Technology*, vol. 26, no. 6, pp. 75–78, 2015.

[2] A.-J. Gao and Y. Liang, "Study on aluminum alloy corrosion and protection under the south sea atmospheric environment," *World Nonferrous Metals*, vol. 32, no. 4, pp. 15–17, 2017.

[3] B. Wang, Z. Wang, G. Cao, Y. Liu, and K. E. Wei, "Localized corrosion of aluminum alloy 2024 exposed to salt lake atmospheric environment in western China," *Acta Metallurgica Sinica*, vol. 50, no. 1, pp. 49–56, 2014.

[4] H. Zhou, X. Li, and C. Dong, "Corrosion behaviors of aluminum alloys in simulated SO_2 pollute atmosphere," *Journal of Aeronautical Materials*, vol. 28, no. 2, pp. 39–45, 2008.

[5] Y. Xiao-Kui, L.-W. Zhang, B. Hu et al., "Corrosion behavior of 7475 high-strength aluminium alloy in marine and rural atmosphere environments," *Surface Technology*, vol. 48, no. 1, pp. 262–267, 2019.

[6] L. Yi, L. Kun, S. Lidong, and T. H. Du, "Corrosion behavior of 3A12, 5052, 6063 aluminum alloys in coastal atmosphere," *Corrosion & Protection*, vol. 40, no. 7, pp. 490–496, 2019.

[7] Y. Shi, *The Electrochemical Studies of Atmospheric Corrosion of Typical Metals*, Zhejiang University, Hangzhou, China, 2008.

[8] A. Ul-Hamid, L. M. Al-Hems, A. Quddus, A. I. Muhammed, and H. Saricimen, "Corrosion performance of aluminium in atmospheric, underground and seawater splatter zone in the northeastern coast of Arabian Peninsula," *Anti-Corrosion Methods and Materials*, vol. 64, no. 3, pp. 326–334, 2017.

[9] C. Qun-zhi, L. Xi-ming, L. Wen-ting et al., "Investigation of corrosion equivalent relationships between the accelerated environment and the typical service environments of aircraft structures," *Acta Aeronautica Et Astronautica Sinica*, vol. 19, no. 4, pp. 414–418, 1998.

[10] C. Qun-Zhi, C. Chang-Jing, Y.-Y. Wang et al., "Study on database of ground corrosion environment of typical airfield," *Equipment Environmental Engineering*, vol. 3, no. 3, pp. 47–49, 2006.

[11] Y.-L. Chen, P. Jin, D.-X. Lin et al., *Structural Corrosion Control and Strength Assessment of Naval Aircraft*, National Defense Industry Press, Beijing, China, 2009.

[12] Y. Xue-Tao, L. Wen-Han, L. Li, X.-J. Zhou, and Z. San-Ping, "Research status of corrosion behavior and anticorrosion measures of aluminum alloy under different climate in China," *Material Protection*, vol. 52, no. 3, pp. 111–116, 2019.

[13] T. Zhang, S. Zhang, H. E. Yu-Ting, B.-L. Ma, and T.-Y. Zhang, "Atmospheric environment demarcation of China based on corrosion of aeronautic metallic materials," *Equipment Environmental Engineering*, vol. 17, no. 5, pp. 1–9, 2020.

[14] China Machinery Industry Federation (CMI), *Corrosion Tests in Artificial Atmospheres—Salt spray tests*, ID: GB/T 10125-2012, 2012.

[15] H. Chun-Ying, S. Chen, L.-S. Wang, B. Zhi-Xiang, B. Sheng-Kai, and L. Sun, "Effect of tartaric acid-sulfuric acid anodizing process parameters on corrosion resistance of LY12 aluminum alloy," *Material Protection*, vol. 51, no. 1, pp. 79–84, 2018.

[16] J. Yang, H. Kuang, C. Fan et al., "Study on corrosion behavior of 2A96 Al alloy in Nacl solution at different time," *Metal Materials and Metallurgy Engineering*, vol. 48, no. 1, pp. 48–52, 2020.

[17] M. Aydın and T. Savaşkan, "Fatigue properties of zinc–aluminium alloys in 3.5% NaCl and 1% HCl solutions," *International Journal of Fatigue*, vol. 26, no. 1, pp. 103–110, 2004.

[18] W.-J. Lee and S.-I. Pyun, "Effects of sulphate ion additives on the pitting corrosion of pure aluminium in 0.01 M NaCl solution," *Electrochimica Acta*, vol. 45, no. 12, pp. 1901–1910, 2000.

[19] S.-T. Zhang, Y. Zhu, W. Yan-Bo, and H. Bao-Rong, "Electrochemical study of inhibitior on aluminium alloy in high concen tration chloride solutions," *Corrosion & Protection*, vol. 27, no. 10, pp. 508–512, 2006.

[20] T. E. Graedel and R. P. Frankenthal, "Corrosion mechanisms for iron and low alloy steels exposed to the atmosphere," *Journal of the Electrochemical Society*, vol. 137, no. 8, 2019.

[21] C. Dong, K. Xiao, L. Xu, H. Sheng, Y. An, and X. Li, "Characterization of 7A04 aluminum alloy corrosion under atmosphere with chloride ions using electrochemical techniques," *Rare Metal Materials and Engineering*, vol. 40, no. S2, pp. 275–279, 2011.

[22] X. Su, *Corrosion Behavior Study of Typical Aluminum Alloy in Simulated Marine Atmospheric Environment*, Hebei University of Engineering, Baoding, China, 2013.

[23] Z. Chen, D. Liang, G. Ma et al., "Influence of UV irradiation and ozone on atmospheric corrosion of bare silver," *Corrosion Engineering, Science and Technology*, vol. 45, no. 2, pp. 169–180, 2010.

[24] T. Ingham, A. Goddard, L. K. Whalley et al., "A flow-tube based laser-induced fluorescence instrument to measure OH reactivity in the troposphere," *Atmospheric Measurement Techniques*, vol. 2, no. 2, pp. 465–477, 2009.